ELSEVIER

Journal of Alloys and Compounds 452 (2008) 127–132

Journal of ALLOYS AND COMPOUNDS

www.elsevier.com/locate/jallcom

First principles calculations of thermodynamic and mechanical properties of high temperature bcc Ta–W and Mo–Ta alloys

K. Masuda-Jindo [a,*], Vu Van Hung [b], N.T. Hoa [b], P.E.A. Turchi [c]

[a] *Department of Materials Science and Engineering, Tokyo Institute of Technology, Nagatsuta 4259, Midori-ku, Yokohama 226-8503, Japan*
[b] *Department of Physics, Hanoi National Pedagogic University, km8 Hanoi-Sontay Highway, Hanoi, Vietnam*
[c] *Lawrence Livermore National Laboratory, PO Box 808, L-353 LLNL, Livermore, CA 94551, USA*

Received 18 September 2006; received in revised form 15 December 2006; accepted 21 December 2006
Available online 12 March 2007

Abstract

The thermodynamic quantities of high temperature metals and alloys are studied using the statistical moment method, going beyond the quasi-harmonic approximations. Including the power moments of the atomic displacements up to the fourth order, the Helmholtz free energies and the related thermodynamic quantities are derived explicitly in closed analytic forms. The configurational entropy term is taken into account by using the tetrahedron cluster approximation of the cluster variation method (CVM). The energetics of the binary (Ta–W and Mo–Ta) alloys are treated within the framework of the first-principles TB-LMTO (tight-binding linear muffin tin orbital) method coupled to CPA (coherent potential approximation) and GPM (generalized perturbation method). The equilibrium phase diagrams are calculated for the refractory Ta–W and Mo–Ta bcc alloys. In addition, the mechanical properties, i.e., temperature dependence of the elastic moduli C_{11}, C_{12} and C_{44} and those of the ideal tensile and shear strengths of the bcc Ta–W and Ta-Mo alloys have been also studied.

Keywords: Statistical moment method; Cluster variation method; TB-LMTO method; Coherent potential approximation; Ta–W and Mo–Ta alloys

1. Introduction

The calculations of the thermodynamic quantities and the equilibrium phase diagrams are of great importance for the purpose of materials designs and developments of high temperature technological alloys. It is the purpose of the present article to study the thermodynamic quantities of metals and alloys using the moment method in the quantum statistical mechanics, hereafter referred to as the statistical moment method (SMM) [1–10]. We firstly derive the Helmholtz free energy $\Psi(V, T)$, of metals and alloys using the fourth order moment approximation, and then calculate the thermodynamic quantities, such as the thermal lattice expansions, root mean square atomic displacements, specific heats, Grüneisen constants and elastic moduli. The application calculations using the SMM will be done for the high temperature bcc alloys, like Ta–W and Mo–Ta systems. Recently, much attention has been paid to alloy systems made of refractory metals of columns VB and VIB of the Periodic Table [11,12], and in particular, Nb, Mo, Ta, and W that display high melting temperature space and nuclear applications. In view of this, we calculate the equilibrium phase diagram of Ta–W and Mo–Ta alloys including the effects of thermal lattice vibrations.

In this paper, we also present a new theoretical scheme on the ideal strengths of metals and alloys including the anharmonicity effects of thermal lattice vibrations on the basis of the statistical moment method (SMM) [1–10]. In analyzing the mechanical properties of materials, especially those of the high temperature materials it is essential to take into account the temperature effects since they depend strongly and sensitively on the temperatures. The ideal tensile and shear strengths are calculated both for the transition elements like bcc Mo and W crystals, and Mo–Ta, Ta–W alloys in comparison with the ordered binary alloys, Fe_3Al and FeAl compounds. It is known that the intermetallic compounds like FeAl alloys have the appealing high-temperature and corrosion resistance properties and they are candidates as novel industrial structural materials [13–15].

The present paper is organized as follows: in Section 2, we present the principles of calculations for the thermodynamic quantities, elastic moduli and ideal strengths of metals and alloys at finite temperatures, including the anharmonicity effects of

* Corresponding author. Tel.: +81 45 924 5636; fax: +81 424 75 0650.
E-mail address: kmjindo@issp.u-tokyo.ac.jp (K. Masuda-Jindo).

0925-8388/$ – see front matter © 2007 Published by Elsevier B.V.
doi:10.1016/j.jallcom.2006.12.163

thermal lattice vibrations. The results of numerical calculations and the related discussions are given in Section 3. The final Section 4 is devoted to the conclusions.

2. Theory

2.1. Effects of thermal lattice vibrations

We derive the thermodynamic quantities of metals and alloys, taking into account the higher (fourth) order anharmonic contributions of the thermal lattice vibrations going beyond the quasi-harmonic (QH) approximation [16]. Within the fourth order moments approximation of the SMM the free energy of the system is given by:

$$\begin{aligned}\Psi &= U_0 + 3N\theta[X + \ln(1 - \mathrm{e}^{-2X})] \\ &\quad + 3N\left\{\frac{\theta^2}{k^2}\left[\gamma_2 X^2 \coth^2 X - \frac{2}{3}\gamma_1\left(1 + \frac{X\coth X}{2}\right)\right]\right. \\ &\quad + \frac{2\theta^3}{k^4}\left[\frac{4}{3}\gamma_2^2 X\coth X\left(1 + \frac{X\coth X}{2}\right)\right. \\ &\quad \left.\left. - 2\gamma_1(\gamma_1 + 2\gamma_2)\left(1 + \frac{X\coth X}{2}\right)(1 + X\coth X)\right]\right\} \quad (1)\end{aligned}$$

where $X = \hbar\omega/2\theta$, θ being $k_\mathrm{B}T$. k and γ_i are second and fourth order vibrational constants [1–10], respectively.

With the aid of the free energy formula $\Psi = E - TS$, one can find the thermodynamic quantities of metals and alloy systems. The specific heats and elastic moduli at temperature T are directly derived from the free energy Ψ of the system. For instance, the isothermal compressibility χ_T is given by:

$$\chi_\mathrm{T} = \frac{3(a/a_0)^3}{[2P + (1/3N)(3\sqrt{3}/4a)(\partial^2\Psi/\partial r^2)_\mathrm{T}]} \quad (2)$$

where

$$\begin{aligned}\frac{\partial^2\Psi}{\partial r^2} &= 3N\left\{\frac{1}{6}\frac{\partial^2 U_0}{\partial r^2} + \theta\left[\frac{X\coth X}{2k}\frac{\partial^2 k}{\partial r^2} - \frac{1}{4k^2}\left(\frac{\partial k}{\partial r}\right)^2\right.\right. \\ &\quad \left.\left.\times\left(X\coth X + \frac{X^2}{\sinh^2 X}\right)\right]\right\} \quad (3)\end{aligned}$$

On the other hand, the specific heats at constant volume C_v is:

$$\begin{aligned}C_v &= 3Nk_\mathrm{B}\left\{\frac{X^2}{\sinh^2 X} + \frac{2\theta}{k^2}\left[\left(2\gamma_2 + \frac{\gamma_1}{3}\right)\frac{X^3\coth X}{\sinh^2 X} + \frac{\gamma_1}{3}\right.\right. \\ &\quad \left.\left.\times\left(1 + \frac{X^2}{\sinh^2 X}\right) - \gamma_2\left(\frac{X^4}{\sinh^2 X} + \frac{2X^4\coth^2 X}{\sinh^2 X}\right)\right]\right\} \quad (4)\end{aligned}$$

The specific heat at constant pressure C_p is determined from the thermodynamic relations:

$$C_p = C_v + \frac{9TV\alpha_\mathrm{T}^2}{\chi_\mathrm{T}} \quad (5)$$

where α_T denotes the linear thermal expansion coefficient and χ_T the isothermal compressibility. The relationship between the isothermal and adiabatic compressibilities, χ_T and χ_s, is simply given by:

$$\chi_\mathrm{s} = \frac{C_v}{C_p}\chi_\mathrm{T} \quad (6)$$

2.2. Cluster variation method and energetics of alloys

The configurational entropies of bcc alloys are calculated using the tetrahedron cluster approximation of the cluster variation method (CVM) [17–19]. The nearest-neighbour and next-nearest-neighbour pair probabilities are taken into account in accordance with the effective pair interaction energies derived from the TB-LMTO-CPA formalism, outlined below. The entropy expression $S^{(N)}$ for bcc lattice is given by:

$$\exp\left(\frac{S^{(N)}}{k}\right) = \frac{(\{\Delta\}_N)^{12}\{\mathrm{Point}\}_N}{(\{\mathrm{Ttrh}\}_N)^6(\{1\mathrm{st}\,n\ Pr\}_N)^4(\{2\mathrm{nd}\,n\ Pr\}_N)^3} \quad (7)$$

In the present study, we will use the so-called generalized perturbation method (GPM) for the energetics of the bcc alloys composed of Ta, Mo and W elements [11,12]. Within the GPM, only the configuration-dependent contribution to the total energy is expressed by an expansion in terms of effective pairwise and multisite interactions. Within the GPM, the ordering contribution to the total energy of an A–B alloy is given by:

$$E(\{p_n^i\}) = E_\mathrm{dis}(c) + \Delta E_\mathrm{ord}(\{p_n^i\}) \quad (8)$$

$$\begin{aligned}\Delta E_\mathrm{ord}(\{p_n\}) &= \sum_{k=1}^{\infty}\frac{1}{k}{\sum_{n_1,\ldots,n_k}}' V^{(k)}_{n_1,\ldots,n_k}\delta c_{n_1}\cdots\delta c_{n_k} \\ &= \frac{1}{2N}\sum_{\substack{ij\\ n,m,n\neq m}} V^{ij(2)}_{nm}\delta c_n^i\delta c_m^j \\ &\quad + \frac{1}{3N}\sum_{\substack{ij\\ n,l,m,\\ n\neq m,m\neq l,n\neq l}} V^{ijk(3)}_{nml}\delta c_n^i\delta c_m^j\delta c_l^k + \cdots \quad (9)\end{aligned}$$

$$V_s^{ij} = -\frac{1}{\pi}\,\mathrm{Im}\int^{E_\mathrm{F}}\mathrm{d}E\sum_{\lambda\mu}G^{\lambda\mu}_{(\mathrm{s})}G^{\mu\lambda}_{(\mathrm{s})}\,\Delta t^\lambda_{ij}\,\Delta t^\mu_{ij},\ldots \quad (10)$$

where δc_{n_i} refers to the fluctuation of concentration on site n_i, $\delta c_{n_i} = p_{n_i} - c$ (c is the concentration in B species), and p_i is an occupation number associated with site n_i, equal to 1 or 0 depending on whether or not site n_i is occupied by a B species. The $V^{(k)}_{n_1,\ldots,n_k}$ corresponds to a kth-order effective cluster interaction (ECI) involving a cluster of k sites.

2.3. Elastic moduli and ideal strengths

We will now present the calculational method of ideal strengths of metals and alloys. Firstly, we consider the bcc crystals and calculate the ideal strength in uniaxial tension along ⟨1 0 0⟩ direction, and then calculate the ideal strength in the shear. In particular we consider the ideal shear strength for the

⟨1 1 1⟩ {1 1 0} slip system, most popular one in the bcc crystal.We employ the calculational procedures of the ideal strengths originally proposed by Frenkel [20] and Orawan [21]. The ideal strength in a given deformation mode is proportional to the elastic modulus that governs linear elastic deformation in that mode. For instance, for the tension in the ⟨1 0 0⟩ direction in bcc crystal, the relevant relaxed elastic modulus is given by:

$$E^{\mathrm{r}}_{\langle 1\,0\,0\rangle} = S^{-1}_{11} = \frac{(C_{11}-C_{12})(C_{11}+2C_{12})}{C_{11}+C_{12}} \tag{11}$$

where S_{ij} and C_{ij} are the elastic compliances and elastic moduli, respectively. In all of the bcc transition metals, the nearest extrema along the tensile deformation path is a maximum corresponding to a fcc structure, i.e., the Bain strain, $\varepsilon_{\mathrm{b}} = 0.26$.

On the other hand, the shear modulus depends sensitively on both the shear direction and the shear plane, but, because of the threefold symmetry for rotation about ⟨1 1 1⟩ in bcc crystal, any shear in a ⟨1 1 1⟩ direction has a common relaxed modulus of:

$$G^{\mathrm{r}}_{\langle 1\,1\,1\rangle} = S^{-1}_{\langle 1\,1\,1\rangle} = \begin{cases} \dfrac{3C_{44}(C_{11}-C_{12})}{4C_{44}+C_{11}-C_{12}} \\ \dfrac{3C_{44}}{1+2A} \end{cases} \tag{12}$$

where the elasticity anisotropy parameter is defined by $A = 2C_{44}/(C_{11}-C_{12})$. Then, for elastically isotropic materials with $A = 1$, one can get the relation $G^{\mathrm{r}}_{\langle 1\,1\,1\rangle} = C_{44}$. The position of the energetic extrema also is nearly identical for all types of shear along ⟨1 1 1⟩ direction [22,23]. This is because of the relatively open structure of bcc, which has eight nearest neighbors at a distance of $0.866a_0$ and six next-nearest neighbors at distance of a_0, where a_0 is the lattice constant. An applied shear breaks the symmetry of these neighbors. Again assuming constant volume deformation for comparative purposes, after a relaxed shear of 0.34, there is a high symmetry crossover point, which is identical for shear on {1 1 2} or {1 2 3} planes. Shear on planes with normals near ⟨1 1 2⟩ or ⟨1 2 3⟩ will also pass through this energetic maximum. A slightly different extrema geometry applies for shears on planes with normals close to ⟨1 1 0⟩ direction [5,6]. Both high symmetry extrema geometries are only reached if full atomic relaxation is allowed.

3. Results and discussions

3.1. Thermodynamic quantities of constituent metals

In Fig. 1, we show the thermal expansion coefficients, α_{v}, of bcc Mo, Ta and W crystals at zero pressure as a function of temperature T, together with the experimental results [24]. The thermal expansion coefficients α_{v} of bcc Mo, Ta and W crystals are shown by dot-dashed, solid and dashed lines, respectively, and they are in good agreement with the corresponding experimental results. In particular, the calculated thermal expansion coefficients of the bcc Ta crystals are in fairly good agreement with the experimental results except for higher temperature region than ∼2000 K. For this higher temperature region, experimental results, by symbols (×) show the anomalous increase of the thermal expansion coefficients as increasing the temperature (which might be attributed to the extrinsic causes such as the oxidisation of the specimen). Instead, the present SMM calculations of the thermal lattice expansion coefficients of bcc Ta crystal (solid curve) are in good agreement with the ab initio theoretical calculations of Ref. [25], symbols (◯), using the anharmonic PIC (particle in a cell) model.

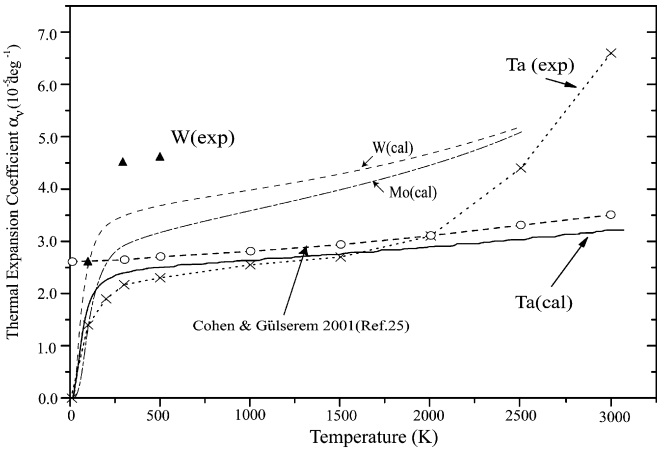

Fig. 1. Thermal lattice expansion coefficients calculated for bcc Mo, Ta and W crystals, in comparison with the experimental results ((▲) for W and (×) for Ta crystals). Also shown by symbols (◯) are ab initio calculation results by Cohen and Gülserem [25].

In Fig. 2, we present the calculated root mean square atomic displacements $\langle u_j^2\rangle$, by solid lines, and root mean square relative displacements $\langle \sigma_j^2\rangle$, by dashed lines, for bcc Mo, Ta and W crystals, as a function of the temperature. The relative magnitudes of $\langle u_j^2\rangle$ and $\langle \sigma_j^2\rangle$ among the bcc elements are such that $\langle u_j^2\rangle_{\mathrm{Ta}} > \langle u_j^2\rangle_{\mathrm{Mo}} > \langle u_j^2\rangle_{\mathrm{W}}$ and $\langle \sigma_j^2\rangle_{\mathrm{Ta}} > \langle \sigma_j^2\rangle_{\mathrm{Mo}} > \langle \sigma_j^2\rangle_{\mathrm{W}}$. For the lower temperature region, i.e., $T \lesssim 1500$ K, both $\langle u_j^2\rangle$ and $\langle \sigma_j^2\rangle$ have the linear temperature dependence, but for higher temperature region, they increase nonlinearly as increasing the temperature. The nonlinear increases of $\langle u_j^2\rangle$ and $\langle \sigma_j^2\rangle$ indicate

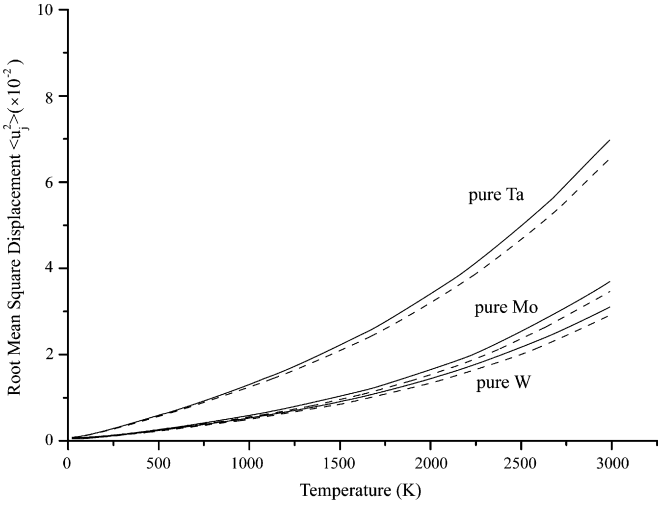

Fig. 2. Temperature dependence of root mean square displacements $\langle u_j^2\rangle$ (solid lines) and root mean square relative displacements $\langle \sigma_j^2\rangle$ (dashed lines) for bcc Mo, Ta and W crystals.

the importance of the anharmonicity of thermal lattice vibrations for the higher temperature region.

3.2. Mo–Ta and Ta–W bcc alloys

To calculate the thermodynamic quantities and the equilibrium phase diagrams of bcc Mo–Ta and Ta–W alloys, we use the cluster variation method (CVM) [17] and the first-principles TB-LMTO method coupled to the coherent potential approximation (CPA) and the generalized perturbation method (GPM) [11,12]. We calculate the change in the free energy $\Delta\Psi$ (eV/atom) due to the inclusion of the thermal vibration effects of bcc Mo–Ta and Ta–W bcc alloys as a function of the temperature T; the concentrations of tantalum are chosen to be 0.0, 0.1, 0.2, 0.25, 0.3, 0.33, 0.4 0.5, 0.6, 0.67, 0.7, 0.8, 0.9 and 1.0. Here, the change in the free energy $\Delta\Psi$ corresponds to the ordering energy defined by "$\Delta E_{\mathrm{ord}} = E_{\mathrm{AA}} + E_{\mathrm{BB}} - 2E_{\mathrm{AB}}$" in the conventional treatments without thermal lattice vibration effects.

The resulting equilibrium phase diagrams of bcc Ta–W alloys are presented in Fig. 3. The dark circles connected by solid lines represent the phase boundaries between B2 and A2 phases of bcc Ta–W alloys, including the thermal lattice vibration effects while the white circles connected by dashed lines are the phase boundaries without including the thermal lattice vibration effects [11,12]. It can be seen in Fig. 3 that the B2 phases of Ta–W alloys are stabilized more strongly by including the anharmonicity effects of thermal lattice vibrations at higher Ta concentration. This theoretical finding is of great interest since the inclusion of the thermal lattice vibration effects is believed in most cases to destabilize the ordered phases as in the CuAu alloys [26]. In addition, we have also calculated the melting temperatures T_{m} (critical temperature of the crystalline stability) of the disordered Mo–Ta and Ta–W alloys using the SMM [1–10], and presented the results of melting temperatures T_{m} of Ta–W alloys in Fig. 3, in comparison with the experimental liquidus (dashed line) and solidus (solid line) curves. Although the direct comparison between the theoretical T_{m} and experimental liquidus and solidus curves is not possible, one sees that there are good correlations between the calculation and experimental results.

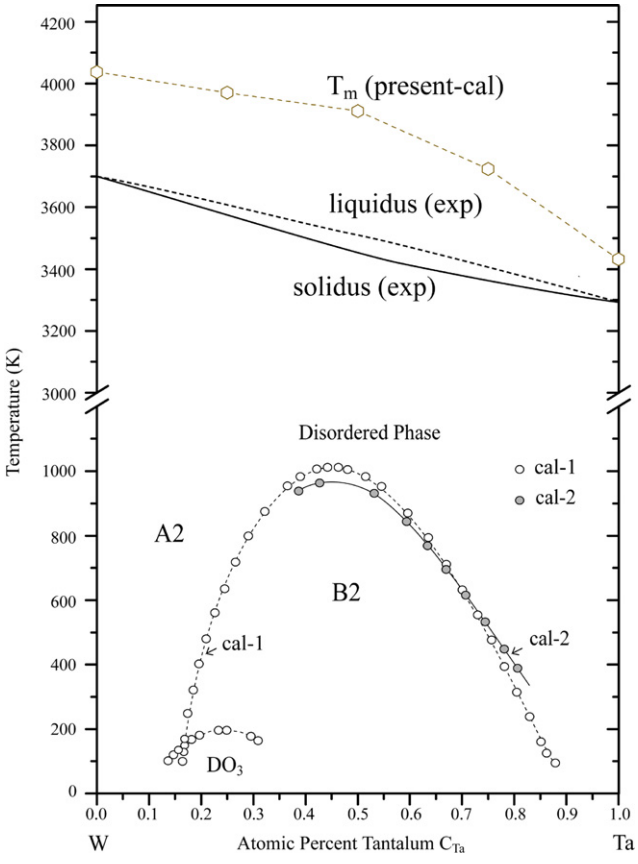

Fig. 3. The calculated equilibrium phase diagram and melting temperatures of Ta–W alloys: cal-2 (cal-1) represent the phase boundaries between B2 and A2 phases, calculated by including (not including) the effects of thermal lattice vibrations.

3.3. Elastic moduli and ideal strength

In Fig. 4, we present the calculated elastic constants C_{11}, C_{12}, C_{44} and bulk modulus B, of bcc W crystal, as a function of the temperature, by using the orthogonal TB d-band approach [27]. One sees in Fig. 4 that the calculated elastic moduli C_{11}, C_{12} and C_{44} of bcc W crystals are in good agreement with the corresponding experimental results [28], especially for lower temperature region. One sees in Fig. 4 that the elastic constants are decreasing function of the temperature, and decreasing rates of C_{11} and C_{12} are considerably larger than those of C_{44}: the decreasing rates of C_{44} are quite small for the whole temperature range. We have also calculated the elastic constants of bcc Mo crystal using the environment dependent sp^3d^5-basis TB method [29] based on the density functional theory (DFT), and found that the calculated features of the elastic constants are quite similar to those obtained by the orthogonal TB method. The elastic constants of bcc Mo crystal are decreasing function of the temperature, and the tendency of the decreasing rates of C_{11}, C_{12}, C_{44} and B are similar to those of bcc W crystal calculated by the orthogonal d-band scheme. The experimental elastic constants of bcc W crystals [28] are presented by symbols (◯) in Fig. 4, but they are limited to lower temperature region than $T = 300$ K, and we

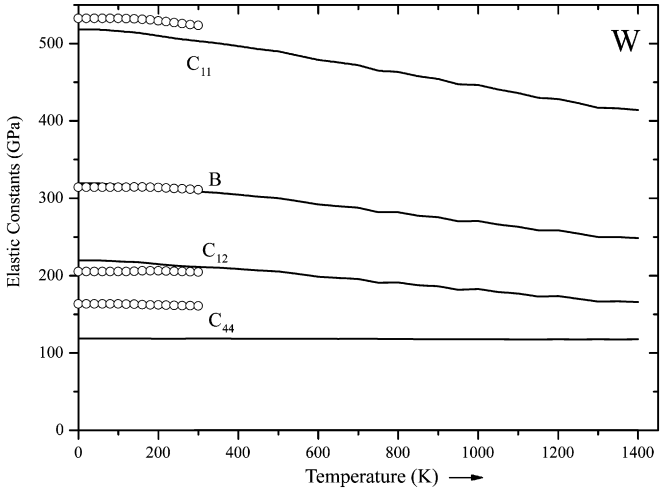

Fig. 4. Temperature dependence of elastic constants, C_{11}, C_{12}, C_{44} and B of bcc W crystal, in units of GPa.

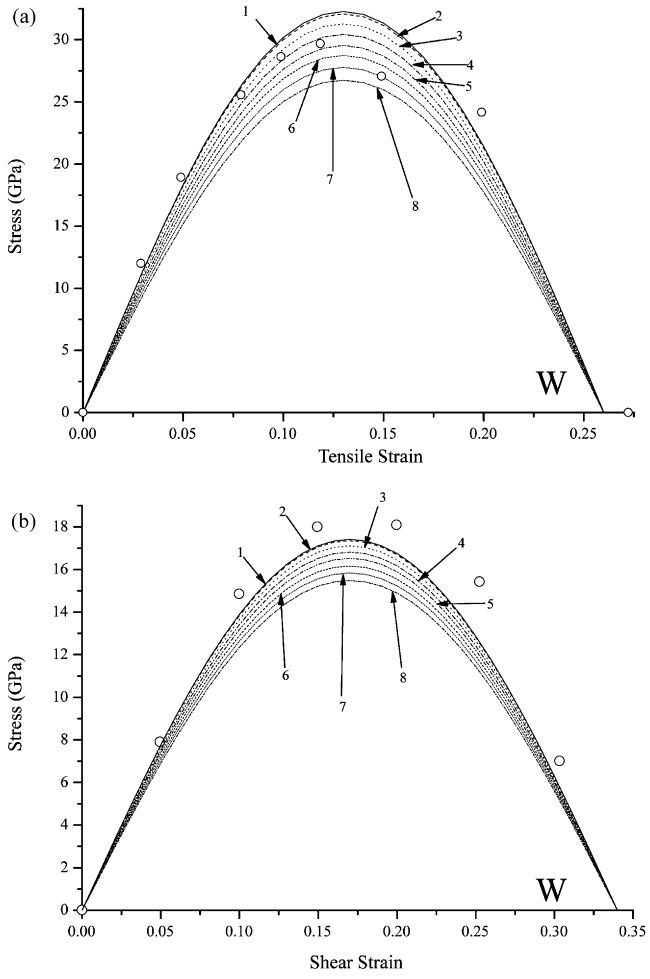

Fig. 5. Tensile and shear strengths of bcc W crystal at $T = 10$ K (1), 100 K (2), 300 K (3), 500 K (4), 700 K (5), 900 K (6), 1100 K (7), and 1300 K (8). Also shown by symbols (◯) are ideal strengths at 0 K, calculated by using ab initio DF theory [22,23].

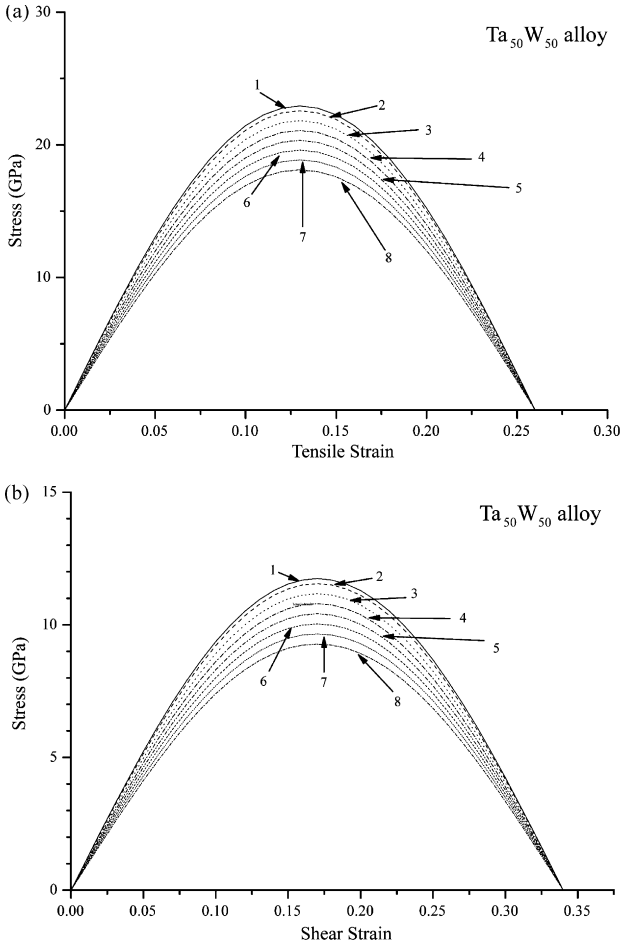

Fig. 6. Ideal tensile and shear strengths of $Ta_{50}W_{50}$ alloy at $T = 10$ K (1), 100 K (2), 300 K (3), 500 K (4), 700 K (5), 900 K (6), 1100 K (7), and 1300 K (8).

can not compare the present theoretical findings (the decreasing rates) of the elastic constants with the experimental observations for higher temperature region. However, we note that the experimental results of the elastic constants of NaCl crystal clearly show the similar tendency of weak temperature dependence of C_{44} as calculated here for bcc Mo and W crystals [30].

The ideal strengths of bcc Mo, Ta and W bcc crystals and Mo–Ta and Ta–W alloys are calculated by using Eqs. (11) and (12) both for the tensile and shear deformations. In Fig. 5, we present the calculated ideal strengths of bcc W crystals. The ideal strengths of $Ta_{50}W_{50}$ bcc alloys are presented in Fig. 6. In both Figs. 5 and 6, the upper (a) and lower (b) figures are the tensile and shear strengths for temperature range 10–1300 K respectively. For bcc Mo, Ta and W crystals and Mo–Ta and Ta–W bcc alloys, the tensile and shear strengths are decreasing function of the temperature, and the tensile strengths are ∼2.0 times larger than those of the shear strengths. In Fig. 6, one sees that both tensile and ideal strengths of bcc $Ta_{50}W_{50}$ alloys become lower (approximately ∼70%) compared to those of bcc W crystal. The decreasing rates of the ideal strengths (with increasing temperatures) of the bcc Mo, Ta and W crystals, and their alloys are considerably larger than those of the intermetallic compounds like Fe_3Al and FeAl [31], which exhibit much lower decreasing rates of the ideal strengths. The calculated ideal strengths are also compared with the experimental results, e.g., tensile tests of nominally dislocation-free "whiskers" and nano-indentation tests on films. Mikhailovskii et al. [32] have studied the tensile fracture of microcrystalline W "whiskers"with diameters in the range 600–2600 Å and along axes parallel to ⟨1 1 0⟩ direction. The maximum strength for W crystal was 28.3 GPa. On the other hand, nano-indentation tests probe the mechanical response to indentation by an indenter that can be no more than a few tens of nanometers in diameter. If the specimen has a low dislocation density, then the nano-indenter may probe essentially defect-free material. If, in addition, the surface of the crystal is treated to prevent premature failure from the interface, then failure may be made to originate in the region of maximum stress beneath the interface. It follows that nano-indentation studies are a promising method for measuring the bulk value of ideal strength. Also shown in Fig. 5 by symbols (◯) are those values calculated by using the ab initio DF theory (at 0 K) [22,23]. The calculated shear strengths of bcc W crystals are shown in Fig. 5(b), together with the previous DFT calculations which can be compared with the experimental shear strengths inferred from nano-indentation experiments, i.e., corrected experimental values of 16.5–18 GPa from 26 to 28 GPa [28,33].

4. Conclusions

We have presented the SMM formalism combined with the CVM and investigated the thermodynamic properties of high temperature bcc metals and alloys composed of Mo, Ta and W elements. The linear thermal expansion coefficients, bulk modulus and root-mean-square atomic displacements are calculated as a function of the temperature as well as a function of the alloy compositions. The calculated results of the thermodynamic quantities are in good agreement with the corresponding experimental results. The equilibrium phase diagrams are calculated for bcc Ta–Mo and Ta–W alloys, including the anharmonicity of thermal lattice vibrations. It has been shown that the B2 phases of Ta–W alloys are stabilized more strongly by including the anharmonicity of thermal lattice vibrations for higher Ta concentration region. The similar tendency has also seen found for Ta–Mo alloys.

Using the free energy formulae derived by the statistical moment method, we have studied the temperature dependence of ideal strengths of metals (Mo, Ta and W) and Ta–Mo and Ta–W alloys. In general, we have found that both tensile and shear strengths of the metals and alloys are decreasing function of the temperature and closely related to the characteristic decreasing behaviors of elastic constants C_{11}, C_{12} and C_{44} of the given crystals: the decreasing rates of elastic constants C_{11} and C_{12} are considerably larger than those of the elastic constant C_{44}. The calculated magnitudes of ideal strengths are in good agreement with the available experimental results.

References

[1] N. Tang, V.V. Hung, Phys. Stat. Sol. B 149 (1988) 511.
[2] N. Tang, V.V. Hung, Phys. Stat. Sol. B 161 (1990) 165;
N. Tang, V.V. Hung, Phys. Stat. Sol. B 162 (1990) 371.
[3] V.V. Hung, K. Masuda-Jindo, J. Phys. Soc. Jpn. 69 (2000) 2067.
[4] V.V. Hung, H.V. Tich, K. Masuda-Jindo, J. Phys. Soc. Jpn. 69 (2000) 2691.
[5] K. Masuda-Jindo, V.V. Hung, J. Phys. Soc. Jpn. 73 (2004) 1205.
[6] K. Masuda-Jindo, V.V. Hung, P.D. Tam, Phys. Rev. B 67 (2003) 094301.
[7] K. Masuda-Jindo, S.R. Nishitani, V.V. Hung, Phys. Rev. B 70 (2004) 184122.
[8] K. Masuda-Jindo, V.V. Hung, M. Menon, Phys. Stat. Sol. (c) 2 (2005) 1781.
[9] V.V. Hung, K. Masuda-Jindo, P.H.M. Hanh, J. Phys.: Condens. Matter 18 (2006) 283.
[10] V.V. Hung, J. Lee, K. Masuda-Jindo, J. Phys. Chem. Solids 67 (2006) 682.
[11] P.E.A. Turchi, A. Gonis, V. Drchal, J. Kudrnocsky, Phys. Rev. B 64 (2001) 085112.
[12] P.E.A. Turchi, V. Drchal, J. Kudmocský, C. Colinet, L. Kaufman, Z.-K. Liu, Phys. Rev. B 71 (2005) 094206;
N.I. Papanicolaou, G.C. Kallinteris, G.A. Evangelakis, D.A. Papaconstantopoulos, Comp. Mater. Sci. 17 (2000) 224.
[13] L. Anthony, J.K. Okamoto, B. Fultz, Phys. Rev. Lett. 70 (1993) 1128.
[14] L.J. Nagel, L. Anthony, J.K. Okamoto, B. Fultz, J. Phase Equilibr. 18 (1997) 551.
[15] R. Besson, J. Morillo, Phys. Rev. B 55 (1997) 193.
[16] V.L. Moruzzi, J.F. Janak, K. Schwarz, Phys. Rev. B 37 (1988) 790.
[17] R. Kikuchi, Phys. Rev. 81 (1951) 988.
[18] R. Kikuchi, K. Masuda-Jindo, Comp. Mat. Sci. 8 (1997) 1.
[19] A. Finel, Prog. Theor. Phys. 59 (Suppl. No. 115) (1994);
A. Finel, R. Tétot, Proc. NATO ASI, Corfu, June, 1995.
[20] J. Frenkel, Z. Phys. 37 (1926) 572.
[21] E. Orowan, Rep. Prog. Phys. 12 (1949) 185.
[22] D. Roundy, C.R. Krenn, M.L. Cohen, Philos. Mag. A 81 (7) (2001) 1725–1747.
[23] C.R. Krenn, D. Roundy, J.W. Morris Jr., M.L. Cohen, Mat. Sci. Eng. A 319–321 (111) (2001) 6.
[24] Y.S. Touloukian, R.K. Kirby, R.E. Taylor, P.D. Desai, Thermophysical Properties of Matter (Thermal Expansion—Metallic Elements and Alloys, vol. 12), Plenum Press, New York, 1975.
[25] R.E. Cohen, O. Gülseren, Phys. Rev. B 63 (2001) 224101.
[26] T. Horiuchi, S. Takizawa, T. Suzuki, T. Mohri, Metall. Mater. Trans. 26 (1995) 11.
[27] K. Masuda, N. Hamada, K. Terakura, J. Phys. F Met. Phys. 14 (1984) 47.
[28] J.P. Hirth, L. Lothe, Theory of Dislocations, McGraw-Hill, New York, 1968;
F.H. Featherston, J.R. Neighbours, Phys. Rev. 130 (1963) 1324.
[29] H. Haas, C.Z. Wang, M. Fähnle, C. Elsasser, K.M. Ho, Phys. Rev. B 57 (1998) 1461.
[30] S.C. Kim, T.H. Kwon, Phys. Rev. B 45 (1992) 2105.
[31] V.V. Hung, K. Masuda-Jindo, N.T. Hoa, in press.
[32] I.M. Mikhaiovskii, P.Y. Poltinin, L.I. Fedorova, Sov. Phys. Solid State 23 (1981) 757.
[33] G. Simmons, H. Wang, Single Crystal Elastic Constants and Calculated Aggregated Properties, MIT Press, Cambridge, 1971.